Durham Tom (Orcid ID: 0000-0001-9473-5195)
Feelisch Martin (Orcid ID: 0000-0003-2320-1158)
Nagy (GUEST EDITOR) Péter (Orcid ID: 0000-0003-3393-235X)

Chemistry, pharmacology and cellular uptake mechanisms of thiometallate sulfide donors

Tom Durham[1], David Zander[1], Niccolò Stomeo[1], Magdalena Minnion[2], Graeme Hogarth[3], Martin Feelisch[2], Mervyn Singer[1], Alex Dyson[1]

[1]Bloomsbury Institute of Intensive Care Medicine, Division of Medicine, University College London, Gower St, London, WC1E 6BT**,** UK.

[2]Clinical and Experimental Sciences, Faculty of Medicine, Southampton General Hospital and Institute for Life Sciences, University of Southampton, Southampton, SO171BJ, UK.

[3]Department of Chemistry, King's College London, Trinity Street, London, SE1 1DB, UK.

Corresponding author:
Alex Dyson; a.dyson@ucl.ac.uk

Key words: tetrathiotungstate; tetrathiomolybdate; anion exchanger-1; persulfide; polysulfide; redox recycling; pharmacokinetics; pharmacodynamics

Short title: Characterisation and cellular uptake mechanisms of thiometallates

This article has been accepted for publication and undergone full peer review but has not been through the copyediting, typesetting, pagination and proofreading process which may lead to differences between this version and the Version of Record. Please cite this article as doi: 10.1111/bph.14670

Abstract

Background and purpose

A clinical need exists for targeted, safe and effective sulfide donors. We recently reported that ammonium tetrathiomolybdate (ATTM) belongs to a new class of sulfide-releasing drugs. Here, we investigate cellular uptake mechanisms of this drug class compared to sodium hydrosulfide (NaHS), and report on the thiometallate tungsten congener of ATTM, ammonium tetrathiotungstate (ATTT).

Experimental approach

In vitro H_2S release was determined by head-space gas sampling of vials containing dissolved thiometallates. Thiometallate and NaHS bioactivity was assessed by spectrophotometry-derived sulfhaemoglobin formation. Cellular uptake dependence on the anion exchanger (AE)-1 was investigated in human red blood cells. ATTM/glutathione interactions were assessed by LC-MS/MS. Rodent pharmacokinetic and pharmacodynamic studies focussed on haemodynamics and inhibition of aerobic respiration.

Key results

ATTM and ATTT both exhibit temperature-, pH-, and thiol-dependence of sulfide release. ATTM/glutathione interactions revealed the generation of inorganic and organic persulfides and polysulfides. ATTM showed greater *ex vivo* and *in vivo* bioactivity over ATTT, notwithstanding similar pharmacokinetic profiles. Cellular uptake mechanisms of the two drug classes are distinct; thiometallates show dependence on the AE-1 channel, while hydrosulfide itself was unaffected by inhibition of this pathway.

Conclusion and implications

Our demonstration that cellular uptake of thiometallates relies upon a plasma membrane ion channel advances our pharmacological knowledge of this drug class. It further supports their utility as cell-targeted sulfide donor therapies. Our results indicate that, as a more stable form, ATTT is better suited as a copper chelator. ATTM, a superior sulfide donor, may additionally participate in intracellular redox recycling.

Non-standard abbreviations

AE-1 – Anion exchanger-1

ATN-224 – Bis-choline tetrathiomolybdate

ATTM – Ammonium tetrathiomolybdate

ATTT – Ammonium tetrathiotungstate

C_{MAX} – Maximum plasma concentration

Deoxy Hb – Deoxyhaemoglobin

GSSH – Glutathione persulfide

GSSSH/GSSSSH – Glutathione polysulfide(s)

H_2DIDS – 4'diisothiocyanato-dihydrostilbene- 2,2'-disulfonic acid

H_2S – Hydrogen sulfide gas

HCl – Hydrochloric acid

HS^- – Hydrosulfide anion

IAM - Iodoacetamide

MoS_4^{2-} – Tetrathiomolybdate ion

MRM – Multiple reaction monitoring

NaHS – Sodium hydrosulfide

Na_2S – Sodium sulfide

Oxy Hb – Oxyhaemoglobin

$PaCO_2$ – Arterial partial pressure of carbon dioxide

PaO_2 – Arterial partial pressure of oxygen

PK/PD – Pharmacokinetics/pharmacodynamics

PVC – Polyvinyl chloride

sHb and Sulf Hb – Sulfhaemoglobin

tHb – Total haemoglobin

WS_4^{2-} – Tetrathiotungstate ion

Bullet-point summary

What is already known

- A clinical need exists for safe and cell-targeted sulfide donors to treat ischaemia/reperfusion injury.
- The copper chelator, ammonium tetrathiomolybdate (ATTM), is a sulfide donor with novel properties.

What this study adds

- We discovered that the cellular uptake mechanism of thiometallates relies on anion exchanger-1 in human erythrocytes.
- ATTM undergoes significant thiol interactions that promote sulfide release and generate per- and polysulfides.

Clinical significance

- Our mechanistic evidence suggests that thiometallates act via a targeted intracellular mechanism of action.
- The potential participation of thiometallates in redox recycling could be applicable to other oxidative pathologies.

Introduction

Hydrogen sulfide (comprising H_2S and HS^-) is the third endogenous gasotransmitter alongside nitric oxide and carbon monoxide, and acts as a signalling molecule across numerous physiological systems (Kimura, 2014; Szabo et al., 2014). Given exogenously in preclinical studies, sulfide protected against diverse pathological conditions, ranging from circulatory (Wang et al., 2011), neurodegenerative (Zhang and Bian, 2014) and arthritic (Wu et al., 2016) disorders to diabetes (Wu et al., 2009), pain (Di Cesare Mannelli et al., 2017) and cancer (Lee et al., 2014). Our particular interest in sulfide relates to its ability to transiently reduce cellular respiration by inhibition of mitochondrial cytochrome C oxidase (Szabo et al., 2014). This, and consequent reduction of mitochondria-derived reactive oxygen species production, confers protection in states of ischaemia/reperfusion injury, hypoxia and circulatory shock (Blackstone and Roth, 2007; Elrod et al., 2007; Morrison et al., 2008).

Notwithstanding more than a decade of promising preclinical research, only a handful of sulfide-based therapies have entered clinical trials (Wallace et al., 2017); none have yet proven successful in randomised phase 2/3 studies. Numerous delivery methods have been investigated, focusing initially on the use of simple sulfur salts such as sodium sulfide (Na_2S). However, these salts release sulfide in a rapid, uncontrolled fashion with resulting implications for safety and efficacy. More recently, drug design of sulfide-based therapeutics has advanced significantly, with identification of numerous slow-release sulfide 'donors' and sulfur-hybrid molecules. These aim for more controlled sulfide delivery and improved targeting to its intended site of action (Szabo and Papapetropoulos, 2017).

We and others recently reported that inorganic thiometallates represent a new class of sulfide-releasing drugs (Xu et al., 2016; Dyson et al., 2017) that confer protection against ischaemia/reperfusion injury (Dyson et al., 2017). Consisting of a transition metal core and four covalently bound sulfur atoms, cleavage of the metal-sulfur bonds enables these molecules to act as slow-release sulfide donors. The archetypical thiometallate, tetrathiomolybdate, was first synthesized nearly 200 years ago (Berzelius, 1826). The ammonium salt, ATTM ($[NH_4]_2MoS_4$), has proven efficacy as a copper chelator, having been developed and used off-label for the treatment of Wilson's disease (Brewer et al., 2009). Notably, the rate(s) of hydrolysis of molecules from this class depend on numerous intrinsic and extrinsic factors (Lee et al., 2007); this ultimately determines their suitability as sulfide

donors or copper chelators.

Given the potential utility of thiometallates for indications not necessarily related to the depletion of copper, we investigated other compounds within this class. Here we report on the chemistry and pharmacology of the tungsten analogue, ATTT ($[NH_4]_2WS_4$), in comparison to its lighter homologue and the 'standard' sulfide generator, NaHS. In view of the need for sulfide mimetics that are better targeted, we explored mechanisms of cellular uptake by both thiometallates and NaHS. We hypothesized that (i) thiometallates utilize non-selective anion channels to gain intracellular access due to their ionic nature in solution and (ii) ATTT would represent a new member of the sulfide-releasing thiometallate drug class. Finally, we elaborate on two methods developed as part of this work, providing a detailed description of our H_2S release assay and the measurement of sulfhaemoglobin, and provide pilot data on the interaction of ATTM with oxidised and reduced glutathione.

Methods

In vitro H_2S release

As noted above, free (biologically active and physiologically relevant) sulfide constitutes H_2S gas and the hydrosulfide (HS^-) anion (May et al., 2018). The assay, developed in-house and described in detail herein, relies on detection of free H_2S that is measured by a commercially available H_2S detector (Z900XP, Environmental Sensors, Boca Raton, FL, USA). Further elaboration on the protocol is provided in Supplement 1. In brief, the compound under investigation is dissolved in phosphate-buffered saline (PBS) to 10x stock solutions and rapidly diluted (0.5 into 4.5 ml) into airtight Falcon tubes (50 ml; Corning Science Mexico, Reynosa, Mexico) containing PBS. The PBS is typically pre-warmed to 37ºC but can be adjusted as necessary (e.g. to different temperatures, pH levels, or to contain thiols, other adjuvants or alternative matrices). Incubate in a water bath (typically for one hour at 37ºC). Withdraw 5 ml of headspace gas over 10 seconds and pass through the detector using a 3-way tap to accommodate the syringe (closed to room air until aspiration of the gas); this is attached to the detector inlet, as depicted in the inset of Fig 1A.

The Z900XP H_2S detector displays a reading every 10 seconds. During the first series of experiments, we recorded both peak H_2S gas levels (in parts per million; ppm), and values during the washout phase until the meter displayed zero. A direct correlation was seen when

comparing the peak H_2S value (Fig 1A) against the sum of the washout readings (decay) over time (area under curve; AUC; Fig 1B). As such, it is appropriate to present only the peak H_2S gas level. In the current study, we adjusted the environment into which thiometallate stocks were diluted as follows: temperature was set to either 4, 21, 37 or 50^{o}C, and solution pH to 4.5, 7.4 or 10. As we previously observed sulfide released by ATTM to be enhanced by the presence of thiols, a further set contained reduced glutathione (5 mmol l^{-1} final concentration). Final concentrations of drug solutions (1-100 mmol l^{-1} total sulfur) and time of incubation (30-180 mins) were also adjusted under standard conditions (pH 7.4, 37^{o}C).

Thiol interactions

We further investigated the interaction of ATTM with glutathione using H_2S generation following incubation with either reduced or oxidised glutathione (GSH and GSSG, respectively; 5 mmol l^{-1}). We additionally monitored the fall in absorbance of ATTM at 468 nm (A_{468}; indicative of breakdown of the molecule and liberation of sulfide) using a microplate reader and BioTek (Gen5) software (Synergy 2, North Star Scientific, Sandy, Beds, UK). For this study, ATTM (175 μmol l^{-1}) ± GSH or GSSG (both 5 mmol l^{-1}) were combined in conditions designed to replicate an intracellular environment (pH 6.8 and 37^{o}C). A_{468} was assessed every 10 min for 800 min. In our final assessment of ATTM/glutathione interactions, the formation of hydrogen disulphide, inorganic polysulfides and organic per/polysulfides (up to S_4) were assessed by LCMS/MS. We additionally studied Na_2S and the oxomolybdate, $[NH_4]_2MoO_4$ as controls. Further details are described in Supplement 2.

Sulfhaemoglobin formation

To assess plasma membrane transport and subsequent intracellular biological activity, we examined the formation of sulfhaemoglobin in blood spiked with either ATTT, ATTM or NaHS. The assay developed and described in detail herein is based on the various forms of haemoglobin (oxy-, deoxy-, carboxy-, met- and sulf-) having distinct absorbance signatures. Fig 2A shows that oxyhaemoglobin is highly absorbent at 541 and 577 nm. The sulfhaemoglobin spectrum, while flatter at these wavelengths, has an additional absorbance peak at 620 nm. Notably, there is no interference from ATTM or ATTT, or the colourless NaHS, at these wavelengths.

Absorbance of any given chromophore is calculated according to the Beer-Lambert law (Fig 2B, *Equation 1*) where *A* is absorbance at a particular wavelength (λ), *c* is concentration of the chromophore, *l* is the pathlength and ε is an extinction co-efficient (known also as millimolar lineic absorbance) specific to the wavelength and chromophore(s) of interest. The contribution of ≥2 chromophores to absorbance can be derived according to *Equation 2* (Fig 2B). For oxy-, deoxy- and sulfhaemoglobin, ε values at 577 and 620 nm are shown in Fig 2C, obtained from Zwart et al., (1981).

Calculation of sulfhaemoglobin can be broadly divided into two components. The first requires an assessment of the relative contributions of oxy- and deoxyhaemoglobin to spectrophotometer-derived total haemoglobin (tHb) measurements in either untreated or baseline samples. This is accomplished using Equation 2 (Fig 2B) and ε values at 577 nm (Fig 2C). To assess the fractions of oxy- and deoxyhaemoglobin, we used a blood gas analyser (ABL90 FLEX, Radiometer, Crawley, West Sussex, UK). In studies where blood gas analyses were not available, the following standard values were used for arterial blood: partial pressure of oxygen (13 kPa), deoxyhaemoglobin (5%), oxyhaemoglobin (95%). The second component concerns manual measurement of spectrophotometer-derived sulfhaemoglobin (sHb) in treated samples, achieved using absorbance and ε values at 620 nm. The fraction of sulfhaemoglobin is then calculated as sHb/tHb that we herein express as a percentage.

We used fresh venous whole blood obtained from consenting healthy human volunteers, collected into ethylenediamine tetraacetic acid (EDTA)-containing (20 ml) syringes (final concentration; 2.5 mmol l^{-1}). This venous blood (typically 15 ml) was subsequently transferred to 50 ml Falcon tubes (with room air in the Falcon headspace) and placed on a rotary shaker for 10 min; this enables oxygenation to a representative arterial partial pressure of oxygen (13 kPa). Whole blood (400 μl) was then incubated with 50 μl of either ATTM, ATTT or NaHS, and 50 μl of PBS. In non-drug treated samples (used both as negative controls and as a reference for total haemoglobin), drug was replaced with PBS. All samples were incubated at 37°C and followed two treatment protocols: a dose-response and a time-course. For the dose-response study, upon dilution in blood, and having accounted for the four sulfur atoms of the thiometallates, final concentrations of total sulfur were 1-100 mmol l^{-1}, with incubation time set at 1 hour. For the time-course, all groups were set at the highest

concentration (100 mmol l^{-1} total sulfur) and incubated for 15-360 minutes. After incubation, a 1/20 dilution in PBS was performed, and 100 μl transferred to 96 well microplates. Absorbance values were derived using the above microplate reader and software, with calculation of sulfhaemoglobin performed as above.

Cellular uptake studies

We considered that the thiometallates would prevail in their respective ionic forms (i.e. MoS_4^{2-}, WS_4^{2-}) upon dissolution. Additionally, the majority (85% at physiological pH and temperature) of the free sulfide generated by NaHS, or liberated by the thiometallates, would be present as the hydrosulfide anion. We thus investigated the role of the human erythrocyte anion-exchanger 1 (AE-1) as a putative cellular uptake mechanism. Whole human blood (400 μl) was pre-treated for 30 min with either 50 μl of the AE-1 inhibitor, H_2DIDS (4'diisothiocyanato-dihydrostilbene-2,2'-disulfonic acid; 0.5 mmol l^{-1}) or an equivalent volume of PBS. Following pre-treatment, 50 μl of either ATTT, ATTM or NaHS were added (100 mmol l^{-1} total sulfur), and samples incubated for either 15 min (NaHS) or 180 min (thiometallates) at 37ºC, prior to measurement of sulfhaemoglobin.

In separate studies using the two thiometallates (1.25 mmol l^{-1}; final concentration), blood samples (with or without H_2DIDS pre-treatment) were incubated for 180 min then centrifuged (14,000 RCF, 1 min). Excess drug was removed by twice substituting the supernatant with an equivalent volume of PBS. Blood cells were then lysed by subjecting samples to three freeze-thaw cycles and filtered to remove plasma membrane fragments and proteins (10 kDa Nominal Molecular Weight Limit microfilters; MerckMillipore, Watford, Herts, UK). Extracellular (from the initial supernatant) and intracellular (following lysis and filtration) drug levels were assessed by spectrophotometry. Absorbance peaks at 392 nm and 468 nm were used, respectively, for ATTT and ATTM, and concentrations determined by comparison against standard curves. Studies were not performed using NaHS as it has no distinct colouration. All experiments utilising H_2DIDS were carried out in amber Eppendorf tubes due to the light sensitivity of this molecule.

Pharmacokinetic/pharmacodynamic (PK/PD) studies

To compare the *in vivo* pharmacology of the thiometallates, we performed PK/PD studies. These experiments were performed according to local ethics committee and UK Home Office

guidelines under the Animals (Scientific Procedures) Act 1986. Male Wistar rats (approximately 300 g body weight) were used as mice markedly reduce their metabolism within hours in response to systemic challenges, whereas rats more closely mimic human responses (Zolfaghari et al., 2013). As drug responses often vary between species, the use of mice would likely confound a translational evaluation of metabolism-modifying agents.

Twelve animals were purchased from Charles River (Margate, Kent UK) and certified healthy and pathogen-free. One week prior to experimentation, animals were housed in standard cages of four individuals on a twelve-hour light/dark cycle, with food and water *ad libitum*. All animals were anaesthetised with isoflurane in room air (Abbott, Maidenhead, Berks, UK); 5% for induction, 2% for surgical procedures and 1.5% for maintenance. They were placed on a heated mat (Harvard Apparatus, Cambridge, Cambs, UK) to maintain rectal temperature at 37°C. The left common carotid artery and right internal jugular vein were cannulated using 0.96 mm outside diameter PVC tubing catheter (Scientific Commodities Inc., Lake Havasu City, AZ, USA). The arterial line was connected to a pressure transducer (Powerlab; AD Instruments, Chalgrove, Oxon, UK) for continuous monitoring of mean arterial blood pressure, and the venous line was used for administration of fluids and drugs. The bladder was cannulated through a keyhole laparotomy to measure urine output and renal excretion of thiometallates. Anaesthesia was then switched to intraperitoneal sodium pentobarbitone (Pentoject; Animalcare, York, Yorks, UK), allowing blood-pressure guided tracheal intubation with 2.08 mm external diameter polythene tubing (Portex Ltd, Hythe, UK) and subsequent mechanical ventilation using a small animal ventilator (Physiosuite, Kent Scientific, Torrington, USA). Ventilator settings were as follows: fraction of inspired oxygen, 0.21; tidal volume, 10 ml kg^{-1}; respiratory rate, 80 min^{-1}; positive end-expiratory pressure, 3 cm H_2O. These settings ensured adequate post-surgical gas exchange and consistent minute volumes across all animals used. Perioperative analgesia was provided by buprenorphine, 0.05 mg kg^{-1} subcutaneously (Reckitt Benckiser, Slough, Berks, UK). In these non-recovery experiments, euthanasia at experiment-end was performed using IV sodium pentobarbitone.

Following surgery and a 1-hour stabilization period, animals received increasing IV bolus doses of ATTT or ATTM (1-100 mg kg^{-1}, n=6 per group). Drugs were dissolved in normal (0.9%) saline and administered (within 2 mins) in a volume of 2 ml kg^{-1} over 10 seconds. H_2S in exhaled breath was monitored by connecting the ventilator exhaust to the (above) H_2S detector. Measurements were collected at baseline, then as follows after each dose: blood

pressure and exhaled H_2S (peak change or level) within 30 seconds, cardiac function (by echocardiography) within 1 min, blood sampling to determine plasma drug concentration at 2 mins, and arterial blood gas analysis (to measure partial pressures of O_2 [PaO_2] and CO_2 [$PaCO_2$], glucose, lactate, and acid/base changes) at 27 mins. Doses were escalated every 30 mins. After the highest dose, the half-life of both drugs was assessed by sampling at 2 mins (for maximal concentration; C_{MAX}) then at regular intervals up to 1 hour post-dose. Urine was collected hourly. Absorbance of plasma or urine samples was assessed using the microplate reader at the wavelength specific to each drug (as above), and concentrations derived by comparison against standard curves. To determine fractional renal excretion, a mass-balance approach was utilised. This was accomplished by calculation of the number of moles of each drug excreted in urine, expressed as a fraction against the number of moles injected.

Data and Statistics

Data are presented as mean ± standard error or median, quartiles, and range. Group sizes were n=5-14 for *in vitro* and human blood studies and n=6 for *in vivo* experiments. Correlations were performed using a non-linear regression, straight line model. Pharmacokinetic data were analysed using a biexponential decay curve and least squares fitting method. Parametric data were analysed using repeated measures one- or two-way ANOVA followed by Bonferroni's *post hoc* testing, as appropriate. Nonparametric data were analysed using the Mann-Whitney U test. All statistical analyses were two-tailed and performed using Prism 7.0.1 software (GraphPad Software, CA, USA; RRID:SCR_002798). All data and statistical analyses comply with recommendations on experimental design and analysis in pharmacology (Curtis et al., 2015). Multiplicity adjusted p-values <0.05 were considered statistically significant.

Materials

We sourced thiometallates (Sigma-Aldrich, Gillingham, Kent, UK) and NaHS (Alfa Aesar, Heysham, Lancs, UK) from specific suppliers as they provide, respectively, good consistency between batches, and the purest form available commercially (Hughes et al., 2009). Although we have found a low level of variability across numerous thiometallate batches, we would urge other researchers to establish their own H_2S release assays if using these molecules as sulfide donors. Particular attention should be drawn to storing and handling these materials in a moisture- and oxygen-free environment. H_2DIDS was obtained from Thermofisher (Hemel Hempstead, Herts, UK). All other chemicals and reagents were obtained from Sigma-Aldrich.

Nomenclature of Targets and Ligands

Key protein targets and ligands in this article are hyperlinked to corresponding entries in http://www.guidetopharmacology.org, the common portal for data from the IUPHAR/BPS Guide to pharmacology (Harding et al., 2018), and are permanently archived in the Concise Guide to pharmacology 2017/18 (Alexander et al., 2017).

Results

In vitro H_2S gas release

We report here the novel finding that ammonium tetrathiotungstate is a new member of the sulfide-releasing inorganic thiometallate drug class. However, it releases only half the amount of free sulfide compared to ATTM under standard incubation conditions (Fig 3A; n=25, pooled data from the control arms of B-F). This pattern was maintained under different experimental environments (all n=5). Both thiometallates release sulfide in a concentration-dependent (Fig 3B; $p<0.05$), and linear fashion over time (Fig 3C; $p<0.05$). Like ATTM, ATTT releases sulfide in a temperature ($p<0.05$), thiol ($p<0.05$) and pH-dependent ($p<0.05$) manner (Fig 3D-F). Warmer and more acidic conditions, and the presence of thiols, promote liberation of sulfide from these molecules.

Thiol interactions

Results of further investigations on the interaction between ATTM and glutathione are shown in Supplementary Fig 1. H_2S generation was significantly enhanced ($p<0.05$) by glutathione, regardless of its oxidation state (Supplementary Fig 1A; n=5). The breakdown kinetics of ATTM were further monitored by temporal decreases in absorbance at 468 nm. Supplementary Fig 1B shows the kinetics of the reaction (untreated; n=14) that were significantly (overall ANOVA; $p<0.05$) enhanced by the addition of either GSH (n=8) or GSSG (n=6). Finally, preliminary data of ATTM/glutathione interactions, at either 21 or 37ºC, revealed the formation of glutathione persulfide (GSSH; S_2) and polysulfides (S_3-S_4; Supplementary Fig 1C); in addition, hydrogen disulfide and inorganic polysulfides were detected (data not shown). Expectedly, this reaction was also observed with Na_2S, while the oxomolybdate, $[NH_4]_2MoO_4$, showed only spontaneous generation of glutathione persulfide that was 2-3 orders of magnitude lower compared to that seen with ATTM; the source of sulfur to form GSSH in these experiments is unclear, but likely originates from metal-driven desulfuration reactions.

Sulfhaemoglobin formation and cellular uptake

We assessed (intracellular) sulfhaemoglobin formation as an indicator of plasma membrane transport to examine cellular uptake mechanisms. All three drugs generated sulfhaemoglobin in a concentration-dependent manner (Fig 4A; n=5). Sulfhaemoglobin formation by the thiometallates was also dependent on time, with ATTM exhibiting significantly ($p<0.05$) more bioactivity than ATTT between 60-360 min (Fig 4B; n=5). By contrast to both ATTM and ATTT, NaHS produced sulfhaemoglobin at significantly ($p<0.05$) higher levels in the dose response study, and significantly ($p<0.05$) quicker in the time-course experiment (Fig 4A-B). Pre-treatment of blood with the AE-1 inhibitor H_2DIDS significantly reduced sulfhaemoglobin formation by both ATTT (Fig 4C; $p<0.05$; n=9) and ATTM (Fig 4D; $p<0.05$; n=6 with H_2DIDS, n=9 without). AE-1 inhibition had no effect on sulfhaemoglobin formation in NaHS-treated samples (Fig 4E; p=0.29; n=7).

The distinct spectral signatures of the thiometallates (Fig 5A) allows for their quantification using basic absorbance assays. To confirm use of the AE-1 transporter by thiometallates using an alternative approach, we assessed disappearance from the plasma of blood treated with these drugs and, in the same samples, the appearance of drugs inside erythrocytes. A similar pattern was observed for both thiometallates, whereby pre-incubation with H_2DIDS reduced both disappearance from plasma (Fig 5B, ATTT; Fig 5C, ATTM; both $p<0.05$; all n=5) and detection of their presence intracellularly (Fig 5D, ATTT, Fig 5E, ATTM; both $p<0.05$; all n=5). The measurement most sensitive to H_2DIDS treatment was the intracellular appearance of the drugs, with AE-1 inhibition reducing ATTT and ATTM concentrations by 73% and 65%, respectively.

To confirm no direct chemical interaction between thiometallates and H_2DIDS in these experiments, we additionally performed a H_2S release assay (n=6; Supplementary Fig 2A) and a spectrophotometric time-course of ATTM absorbance (n=6; Supplementary Fig 2B) with and without H_2DIDS. These results showed no chemical interaction between these molecules (p=0.97 and 0.98, respectively).

PK/PD studies

Eleven of the twelve studied animals survived until the end of the experiment protocol. One (ATTM-treated) animal died from an accidental air embolus. Final group sizes were 6 for ATTT and 5 for ATTM. Both thiometallates caused a dose-dependent metabolic acidaemia,

evidenced by falls in arterial pH (Fig 6A) and base excess (the metabolic component of acid-base interactions; Fig 6B). No changes in the respiratory component, arterial $PaCO_2$, were observed in these mechanically ventilated animals (Fig 6C). The magnitude of these metabolic changes was significantly ($p<0.05$) pronounced in ATTM-treated animals; this was mirrored by a dose-dependent rise in blood lactate (Fig 6D; $p<0.05$) and fall in blood glucose (Fig 6E; $p<0.05$), indicative of a compensatory increase in glycolysis (anaerobic respiration). ATTT-treated animals only showed a rise in arterial lactate at the highest dose (Fig 6D) and this was not accompanied by any change in blood sugar (Fig 6E). Dose-dependent falls in blood pressure (Fig 6F) were observed only at supra-pharmacological doses ($\geq$30 mg kg^{-1}). However, this reduction was transient (typically <2 minutes), did not differ significantly between drugs ($p=0.34$), and did not impact upon cardiac output at any dose level (Fig 6G; $p=0.12$). No exhaled H_2S was detected over the dose-range studied.

In order to determine if the pharmacodynamic differences between thiometallates (i,e, greater potency with ATTM) were due to differences in drug handling, we performed pharmacokinetic analyses (Fig 7). Colouration of the thiometallates allowed for their quantification in blood and urine. Plasma concentrations of both drugs followed a direct linear correlation with the quantity administered in the dose range 1-100 mg kg^{-1} (Fig 7A). Assessment of the half-life following administration of the highest dose revealed, as discovered previously for ATTM, a bi-exponential decay in plasma concentrations for both thiometallates (Fig 7B). Half-lives were calculated for the fast (distribution) and slow (elimination) phases of these decay curves. These were, respectively, 1.28 and 23.4 min for ATTT, compared with 1.36 and 21.5 min for ATTM. An assessment of urine volume (Fig 7C; $p=0.93$) and the number of moles in urine (data not shown) showed comparable results for ATTT and ATTM. Accordingly, percentage renal excretion was similar for both compounds (ATTT, 0.59±0.11%; ATTM, 0.67±0.23%; $p=0.75$). Using acidification of the blood as a biomarker of mitochondrial inhibition, PK/PD analysis (Fig 7D) demonstrated that ATTM was twice as potent as ATTT; the PK/PD slope, i.e the relationship of plasma drug concentration to blood acidification (reduction in pH), was 0.14±0.02 for ATTM and 0.07±0.01 for ATTT ($p<0.05$).

Discussion

The putative therapeutic utility of thiometallates has been investigated for over 40 years. The most frequently studied drug in this class, ATTM, has demonstrated preclinical efficacy in >10 diverse disease pathologies ranging from its initial indication, Wilson's disease, to Alzheimer's disease, pain and cancer (Brewer, 2009, 2014). These studies assumed the mechanism of action to be via copper chelation, with examples including the depletion of injurious levels of copper in Wilson's disease, to reduction of copper-dependent angiogenesis by solid tumours. However, in addition to its modulation of copper status, we and others recently reported ATTM to be a slow-release sulfide donor (Xu et al., 2016; Dyson et al., 2017).

Interest in sulfide as a potential therapeutic surged following publication in 2005 of a landmark study in which mice breathing H_2S entered a profound and reversible 'suspended animation-like state' (Blackstone et al., 2005). However, unsuccessful clinical trials using basic sulfur salts encouraged the notion that delivery of sulfide needs to be better targeted. This drove the design of more sophisticated sulfide-releasing molecules (Szabo and Papapetropoulos, 2017; Yang et al., 2017) that, once activated, aim to release sulfide in a more controlled manner. We contended that the combination of chemically and biologically relevant factors promoting sulfide release by ATTM are unique (Dyson et al., 2017). These characteristics help to ensure that sulfide release is better targeted to its intended intracellular site of action. Coupled with the historical use of this drug class over many decades in humans, this has led us to investigate its utility in modifying reperfusion injury in a clinically relevant setting.

Given this therapeutic potential of ATTM, we explored other molecules within this drug class and, as remains largely unknown for other sulfide donors, potential mechanisms of cellular uptake. We examined the tungsten congener of ATTM and, in line with our hypothesis, we confirmed ATTT also acts as a sulfide donor. In accordance with the similarities in chemical composition, and the proximity of molybdenum and tungsten in the periodic table, several parallels were seen with regard to their sulfide-release profile. ATTT releases sulfide in a controlled fashion over time when dissolved in aqueous solution and, like ATTM, this is accelerated by heat, acidity, and the presence of thiols. However, across this wide range of environmental conditions, ATTT releases only around half the quantity of sulfur as sulfide

compared to ATTM. In keeping with our findings, Lee et al., (2007) demonstrated that rates of hydrolysis of ATTT, at various pH levels, are significantly slower than those of ATTM. Hydrolysis of thiometallates, particularly in acidic environments, generates a vast array of polynuclear species. For example, following dilution of ATTM with equimolar HCl, the most abundant form (>40%) was the polynuclear anion, $Mo_3S_9^{2-}$, and this trimeric formation liberates free sulfide (Quagraine et al., 2009).

Unlike hydrolysis, the mechanism(s) of enhanced sulfide release from thiometallates by thiols requires further study. Focussing on ATTM, we expand on our previous findings here by demonstrated that not only reduced thiols but also their oxidised forms (shown here with GSSG) promote the release of sulfide from thiometallates. It is notable that ATTM and ATTT lie on a redox knife edge; they have highly oxidised metal centres bound to electron-rich (and hence oxidisable) ligands and, as such, are able to interact with other compounds in a variety of redox states. In preliminary experiments, we show that ATTM can interact with thiols to generate hydrogen disulfide and glutathione persulfide, as well as organic and inorganic polysulfides. These findings enrich our knowledge base of ATTM; beyond acting as a metabolic-modulating sulfide donor via partial inhibition of cytochrome C oxidase, 'bioactivation' of thiometallates by thiols, with subsequent per- and polysulfide formation, raises the potential for significant interactions that concern intracellular redox biology. With regard to the putative efficacy of this compound for oxidative pathologies such as ischaemia/reperfusion injury, the ability of ATTM to react with oxidised thiols to generate powerful reducing molecules (intracellular redox recycling) is a novel, tantalising and intriguing aspect of its molecular mode of action. The importance of this feature in physiolgical and pathophysiological settings will be subject to further investigation.

In view of the increased appreciation of the need for cell-targeted sulfide donors, there is a surprisingly small literature on cellular uptake mechanisms. Although there are considerable biological differences between water and gaseous sulfide, their similarity in chemical structure prompted exploration of the ability of H_2S to use plasma membrane aquaporins (Mathai et al., 2009). The authors found that no facilitator was required, and, in accordance with the known lipid solubility of sulfide, concluded that simple diffusion occurs without enablement by membrane channels (Mathai et al., 2009). However, physiologically relevant free sulfide is maintained in equilibrium in two forms; $H_2S \leftrightarrow HS^-$ with a pKa value of 6.76 (Liu et al., 2012). This dictates around 85% of physiological sulfide is present as the

hydrosulfide anion. As such, (and, notably, in addition to free diffusion) a role for the most ubiquitous ion transporter in human erythrocytes, the anion exchanger-1, has been suggested (Jennings, 2013).

The mechanism of cellular uptake by thiometallates has not been previously explored. Further to the rationale for studying transfer of sulfide by ion exchange, the ionic nature of ATTT and ATTM following dissolution suggested an anion exchanger would be a strong candidate. We initially used formation of intracellular sulfhaemoglobin in intact human erythrocytes as a surrogate of plasma membrane transport. Accordingly, pre-incubation of human blood with the AE-1 inhibitor, H_2DIDS prevented, at least in part, the formation of sulfhaemoglobin. Not surprisingly native sulfide (from NaHS) did not exclusively use this channel as diffusion permits rapid cellular entry (Jennings, 2013). To confirm the role of the AE-1 exchanger in cellular thiometallate uptake, we also measured intra- and extracellular concentrations of these drugs using a basic absorbance assay. H_2DIDS treatment reduced both extracellular disappearance and intracellular detection of both thiometallates. Given that the formation of sulfhaemoglobin could not be fully prevented, it is conceivable that some free extracellular sulfide cleaved from these molecules may gain access by diffusion and contribute to its formation. Other ion channels and/or additional unstudied mechanisms may also be involved. However, given the substantial inhibition (65-73%) of intracellular detection, we consider that the AE-1 exchanger is an important mechanism governing the targeted intracellular delivery of this class of drugs.

Although we focussed our attention on the human erythrocyte AE-1 exchanger, this channel is present in various forms elsewhere (Walsh and Stewart, 2010; Redzic, 2011), including the α-intercalated cells of the kidney, endothelial cells of the blood brain barrier and a truncated variant in rat heart. This suggests that the AE-1 exchanger uptake mechanism may be relevant for other target tissues.

As we have previously assessed the utility of thiometallates for the putative treatment of reperfusion injury, we examined the pharmacology of ATTT and ATTM *in vivo*, with a particular focus on haemodynamics and biomarkers of inhibition of aerobic respiration. The known hypotensive effect of sulfide-releasing drugs, particularly at high concentrations, was observed here. This is attributed to free circulating sulfide that occurs via multiple putative

mechanisms described in detail elsewhere (Liu et al., 2012). However, this hypotensive effect was transient in nature (<2 mins), only presented with supra-pharmacological dosing, and occurred in the absence of detectable exhaled H_2S (indicative of high quantities of free circulating sulfide).

We monitored blood acid/base status and lactate levels as biomarkers of mitochondrial electron transport chain inhibition. By inhibiting oxidative phosphorylation, cells augment both net ATP hydrolysis and glycolysis. Both of these processes release H^+ ions that contribute to (metabolic) acidaemia, and the latter to an excess of glycolysis-derived pyruvate that, unable to enter the mitochondrion, undergoes dehydrogenation to lactate. Given the enhanced stability profile of ATTT, these effects were less pronounced than those observed with ATTM. We confirmed that these metabolic disparities were not due to differences in drug handling. There was a remarkably similar pharmacokinetic profile for both drugs; on comparison of the PK/PD relationship, we show that ATTM is twice as potent as a modulator of oxidative respiration.

The proposed mechanism of copper chelation by the thiometallates is formation of a tripartite complex between the thiometallate anion, a metal (mainly copper, but to a lesser extent, iron, cobalt and other metal ions) and a protein (e.g albumin) (Hou et al., 2007). In addition to the nature of the metal, hydrolysis rates of these molecules are also determined by the cation (Lee et al., 2007). In a previous study we showed that ATN-224, the bis-choline salt of tetrathiomolybdate, released less sulfide compared to ATTM *in vitro* (Dyson et al., 2017). As a result, it was less effective as a metabolic modulator *in vivo.* This is considered desirable for ATN-224 as it is undergoing clinical development as a copper-sequestering agent for Wilson's disease and shows some utility for cancer (Lowndes et al., 2008; Brewer, 2009, 2014). Our results here suggest that ATTT falls into the same category as ATN-224, being better suited as a copper chelator over a sulfide donor. While this could potentially lessen its utility in ischaemia/reperfusion injury, hypoxia and circulatory shock states, it could provide additional benefit in pathologies sensitive to depletion of copper.

With respect to ATTM, we have identified a safe and effective lead candidate for the treatment of ischaemia/reperfusion injury. Its sulfide release profile is better suited to this indication over other molecules (ATTT, bis-choline tetrathiomolybdate) within this class. Importantly, given the appreciated need for sulfide drugs that are better targeted, we have

demonstrated for the first time that thiometallates use non-selective ion transporters to gain access to intracellular compartments. Moreover, the sulfide release profile of these drugs (sensitive to thiols and low pH) dictates that more sulfide be released intracellularly, particularly in ischaemic cells that exhibit lower intracellular pH levels and have a greater need for treatment.

Author contributions

Experimental work: TD, DZ, NS, MM, AD
Wrote manuscript: TD, MM, MF, MS, AD
Data analysis and statistics: TD, AD
Conception, design and supervision: AD
Academic input and knowledge transfer: GH, MM, MF, MS, AD
Read and approved final manuscript: All authors

Conflict of interest

AD and MS are developing thiometallates for the treatment of reperfusion injury

Declaration of transparency and scientific rigour

This Declaration acknowledges that this paper adheres to the principles for transparent reporting and scientific rigour of preclinical research as stated in the *BJP* guidelines for Design & Analysis, and Animal Experimentation, and as recommended by funding agencies, publishers and other organisations engaged with supporting research.

Acknowledgements

We acknowledge Dr Alireza Mani (University College London, UK) for his advice regarding micropore filters and assessment of intracellular drug levels and Prof Mike Jennings (University of Arkansas, USA) for advice on the preparation and use of H_2DIDS.

References

Alexander SPH, Kelly E, Marrion NV, Peters JA, Faccenda E, Harding SD, Pawson AJ, Sharman JL, Southan C, Davies JA; CGTP Collaborators. (2017) The Concise Guide to PHARMACOLOGY 2017/18: Transporters. Br J Pharmacol. 174 Suppl 1: S360-S446.

Berzelius, J.J. (1826). Ueber die Schwefelsalze. Annalen der Physik *83*: 261–288.

Blackstone, E., Morrison, M., and Roth, M.B. (2005). H_2S induces a suspended animation–like state in mice. Science *308*: 518–518.

Blackstone, E., and Roth, M.B. (2007). Suspended animation-like state protects mice from lethal hypoxia. Shock *27*: 370–372.

Bogdándi, V., Ida, T., Sutton, T.R., Bianco, C., Ditrói, T.,1, Koster, G. (2018) Speciation of reactive sulfur species and their reactions with alkylating agents: do we have any clue about what is present inside the cell? Br J Pharmacol. doi: 10.1111/bph.14394. [Epub ahead of print]

Brewer, G.J. (2009). The use of copper-lowering therapy with tetrathiomolybdate in medicine. Expert Opin Investig Drugs*18*: 89–97.

Brewer, G.J. (2014). The promise of copper lowering therapy with tetrathiomolybdate in the cure of cancer and in the treatment of inflammatory disease. J Trace Elem Med Biol *28*: 372–378.

Brewer, G.J., Askari, F., Dick, R.B., Sitterly, J., Fink, J.K., Carlson, M., et al. (2009). Treatment of Wilson's disease with tetrathiomolybdate: V. control of free copper by tetrathiomolybdate and a comparison with trientine. Transl Res *154*: 70–77.

Curtis, M.J., Bond, R.A., Spina, D., Ahluwalia, A., Alexander, S.P.A., Giembycz, M.A., et al. (2015). Experimental design and analysis and their reporting: new guidance for publication in BJP. Br J Pharmacol *172*: 3461–3471.

Di Cesare Mannelli, L., Lucarini, E., Micheli, L., Mosca, I., Ambrosino, P., Soldovieri, M.V., et al. (2017). Effects of natural and synthetic isothiocyanate-based H_2S-releasers against chemotherapy-induced neuropathic pain: Role of Kv7 potassium channels. Neuropharmacol *121*: 49–59.

Dyson, A., Dal-Pizzol, F., Sabbatini, G., Lach, A.B., Galfo, F., Santos Cardoso, J. dos, et al. (2017). Ammonium tetrathiomolybdate following ischemia/reperfusion injury: Chemistry, pharmacology, and impact of a new class of sulfide donor in preclinical injury models. PLOS Med *14*: e1002310.

Elrod, J.W., Calvert, J.W., Morrison, J., Doeller, J.E., Kraus, D.W., Tao, L., et al. (2007). Hydrogen sulfide attenuates myocardial ischemia-reperfusion injury by preservation of mitochondrial function. Proc. Natl. Acad. Sci. U.S.A. *104*: 15560–15565.

Harding SD, Sharman JL, Faccenda E, Southan C, Pawson AJ, Ireland S et al. (2018). The IUPHAR/BPS Guide to PHARMACOLOGY in 2018: updates and expansion to encompass the new guide to IMMUNOPHARMACOLOGY. Nucl Acids Res 46: D1091-D1106.

Hou, G., Dick, R., Zeng, C., and Brewer, G.J. (2007). Antitumor and antiinflammatory effects of tetrathiotungstate in comparison with tetrathiomolybdate. Transl Res *149*: 260–264.

Hughes, M.N., Centelles, M.N., and Moore, K.P. (2009). Making and working with hydrogen sulfide. Free Rad Biol Med *47*: 1346–1353.

Jennings, M.L. (2013). Transport of H_2S and HS^- across the human red blood cell membrane: rapid H_2S diffusion and AE1-mediated Cl^-/HS^- exchange. Am J Physiol Cell Physiol *305*: C941–C950.

Kimura, H. (2014). Production and Physiological Effects of Hydrogen Sulfide. Antiox Redox Signal *20*: 783–793.

Lee, V.E., Schulman, J.M., Stiefel, E.I., and Lee, C.C. (2007). Reversible precipitation of bovine serum albumin by metal ions and synthesis, structure and reactivity of new tetrathiometallate chelating agents. J Inorg Biochem *101*: 1707–1718.

Lee, Z.W., Teo, X.Y., Tay, E.Y.W., Tan, C.H., Hagen, T., Moore, P.K., et al. (2014). Utilizing hydrogen sulfide as a novel anti-cancer agent by targeting cancer glycolysis and pH imbalance. Br J Pharmacol *171*: 4322–4336.

Liu, Y.-H., Lu, M., Hu, L.-F., Wong, P.T.-H., Webb, G.D., and Bian, J.-S. (2012). Hydrogen Sulfide in the Mammalian Cardiovascular System. Antiox Redox Sign *17*: 141–185.

Lowndes, S.A., Adams, A., Timms, A., Fisher, N., Smythe, J., Watt, S.M., et al. (2008). Phase I Study of Copper-Binding Agent ATN-224 in Patients with Advanced Solid Tumors. Clinical Cancer Research *14*: 7526–7534.

Mathai, J.C., Missner, A., Kugler, P., Saparov, S.M., Zeidel, M.L., Lee, J.K., et al. (2009). No facilitator required for membrane transport of hydrogen sulfide. Proc. Natl. Acad. Sci. U.S.A. *106*: 16633–16638.

May, P.M., Batka, D., Hefter, G., Königsberger, E., Rowland D. (2018) Goodbye to S_2^- in aqueous solution. Chem. Commun. *54*: 1980–1983.

Morrison, M.L., Blackwood, J.E., Lockett, S.L., Iwata, A., Winn, R.K., and Roth, M.B. (2008). Surviving blood loss using hydrogen sulfide. J Trauma *65*: 183–188.

Quagraine, E., Georgakaki, I., and Coucouvanis, D. (2009). Reactivity and kinetic studies of $[NH_4]_2MoS_4$ in acidic aqueous solution: Possible relevance to the angiostatic function of the MoS_4^{2-} ligand. J Inorg Biochem *103*: 143–155.

Redzic, Z. (2011). Molecular biology of the blood-brain and the blood-cerebrospinal fluid barriers: similarities and differences. Fluids and Barriers of the CNS *8*: 3.

Szabo, C., and Papapetropoulos, A. (2017). International Union of Basic and Clinical Pharmacology. CII: Pharmacological Modulation of H_2S Levels: H_2S Donors and H_2S Biosynthesis Inhibitors. Pharmacol Rev *69*: 497–564.

Szabo, C., Ransy, C., Módis, K., Andriamihaja, M., Murghes, B., Coletta, C., et al. (2014). Regulation of mitochondrial bioenergetic function by hydrogen sulfide. Part I. Biochemical

and physiological mechanisms: Biochemistry of H_2S and mitochondrial function. Br J Pharmacol *171*: 2099–2122.

Wallace, J.L., Vaughan, D., Dicay, M., MacNaughton, H.K., and Nucci, G. de (2017). Hydrogen Sulfide-Releasing Therapeutics: Translation to the Clinic. Antiox Redox Signal. *28*: 1533-1540.

Walsh, S.B., and Stewart, G.W. (2010). Anion exchanger 1: Protean function and associations. Int J Biochem Cell Biol *42*: 1919–1922.

Wang, X., Wang, Q., Guo, H., and Zhu, H.Z. (2011). Hydrogen sulfide attenuates cardiac dysfunction in a rat model of heart failure: a mechanism through cardiac mitochondrial protection. Biosci Rep *31*: 87–98.

Wu, L., Yang, W., Jia, X., Yang, G., Duridanova, D., Cao, K., et al. (2009). Pancreatic islet overproduction of H_2S and suppressed insulin release in Zucker diabetic rats. Lab Invest *89*: 59–67.

Wu, W.-J., Jia, W.-W., Liu, X.-H., Pan, L.-L., Zhang, Q.-Y., Yang, D., et al. (2016). S-propargyl-cysteine attenuates inflammatory response in rheumatoid arthritis by modulating the Nrf2-ARE signaling pathway. Redox Biol *10*: 157–167.

Xu S., Yang C.-T., Meng F.-H., Pacheco A., Chen L., and Xian M. (2016) Ammonium tetrathiomolybdate as a water-soluble and slow-release hydrogen sulfide donor. Bioorganic & Medicinal Chemistry Letters *26*: 1585–1588.

Yang, C., Chen, L., Xu, S., Day, J.J., Li, X., and Xian, M. (2017). Recent Development of Hydrogen Sulfide Releasing/Stimulating Reagents and Their Potential Applications in Cancer and Glycometabolic Disorders. Front Pharmacol *8*: 664.

Zhang, X., and Bian, J.-S. (2014). Hydrogen Sulfide: A Neuromodulator and Neuroprotectant in the Central Nervous System. ACS Chem Neurosci *5*: 876–883.

Zhao, Y., Kang, J., Park, C.-M., Bagdon, P.E., Peng, B., and Xian, M. (2014). Thiol-Activated gem-dithiols: a new class of controllable hydrogen sulfide donors. Org Lett *16*: 4536–4539.

Zolfaghari, P.S., Pinto, B.B., Dyson, A., and Singer, M. (2013). The metabolic phenotype of rodent sepsis: cause for concern? Intensive Care Med Exp *1*: 25.

Zwart, A., Buursma, A., Kampen, E.J. van, Oeseburg, B., Ploeg, P.H. van der, and Zijlstra, W.G. (1981). A multi-wavelength spectrophotometric method for the simultaneous determination of five haemoglobin derivatives. J. Clin Chem Clin Biochem. *19*: 457–463.

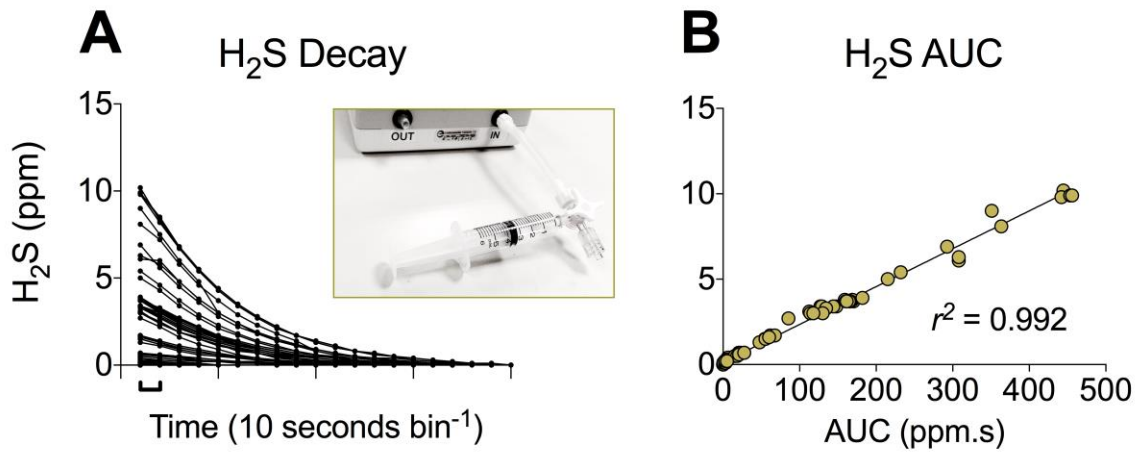

Fig 1. H_2S release test. Comparison of (A) H_2S values over time and (B) the area under curve (AUC) during washout. Inset picture in (A) shows the apparatus for H_2S detection. Values recorded are in parts per million (ppm).

A

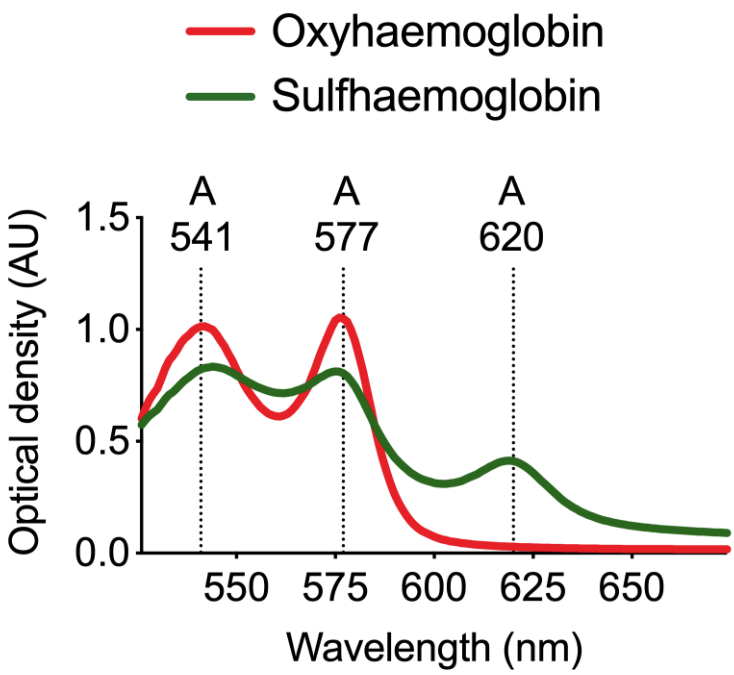

B

$$A^{\lambda} = \varepsilon^{\lambda}.c.l \qquad (1)$$

$$A^{\lambda} = \varepsilon_1^{\lambda}.c_1.l + \varepsilon_2^{\lambda}.c_2.l + \ldots \varepsilon_n^{\lambda}.c_n.l \qquad (2)$$

C

λ (nm)	Deoxy Hb	Oxy Hb	Sulf Hb
577	9.4	15.4	8.1
620	1.23	0.24	20.8

Fig 2. Sulfhaemoglobin assay. (A) spectrophotometry-derived absorbance spectrum of oxyhaemoglobin and sulfhaemoglobin. (B) shows equations for the calculation of absorbance for (1) one, and (2) an infinite number (n) of dissolved chromophores. (C) extinction coefficients for deoxyhaemoglobin, oxyhaemoglobin, and sulfhaemoglobin (Zwart et al., 1981). Coefficients required for calculation of total- and sulfhaemoglobin are shown in shaded cells. λ, wavelength.

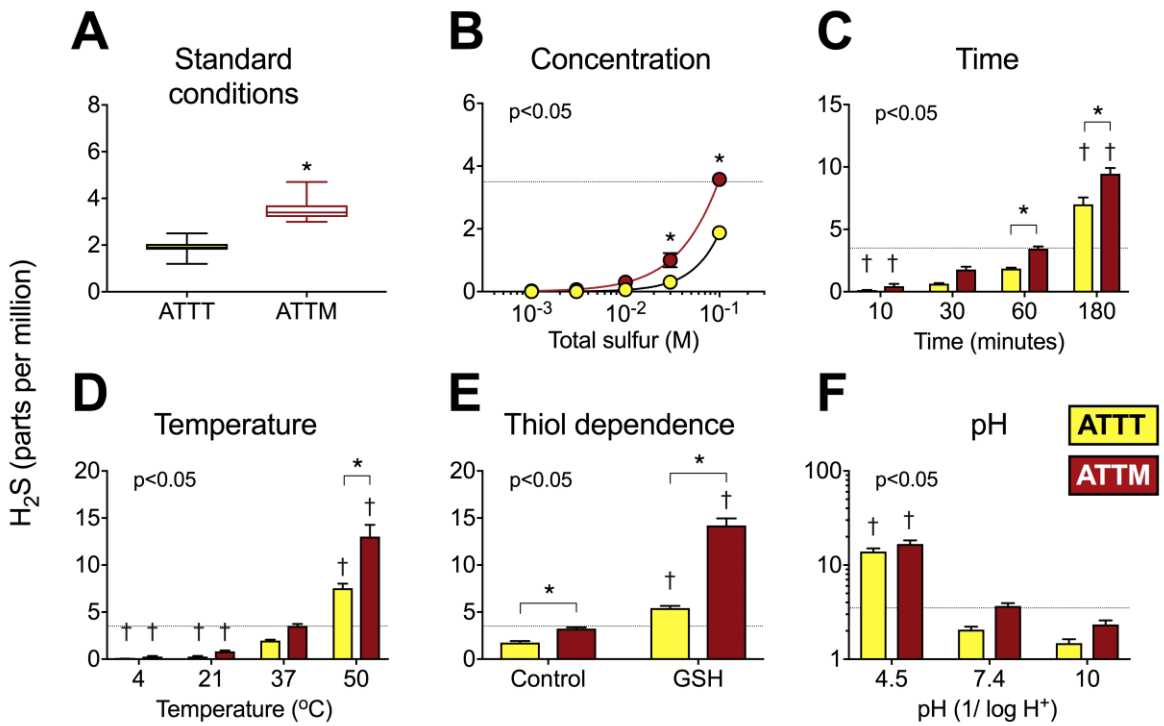

Fig 3. In vitro H_2S release from ATTM and ATTT under different experimental conditions. In (A), standard conditions indicate that drugs (100 mmol l^{-1} total sulfur; n=25; pooled data from the control arms of B-F) were incubated for 1h at physiological pH (7.4) and temperature (37°C). (B) shows concentration dependence of drugs incubated for 1h (n=5). Effects of time, temperature, the presence of thiols (reduced glutathione, GSH) and variations in pH are shown, respectively, in (C-F); all n=5. The dotted lines reflect typical H_2S gas levels (4 ppm) obtained from ATTM (100 mmol l^{-1} total sulfur) following 1h incubation at normal physiological pH and temperature. Statistics: 2-way ANOVA followed by Bonferroni's test. Stated p-values are the result of overall ANOVA. *p<0.05 between ATTM and ATTT and †p<0.05 for each drug compared to standard conditions.

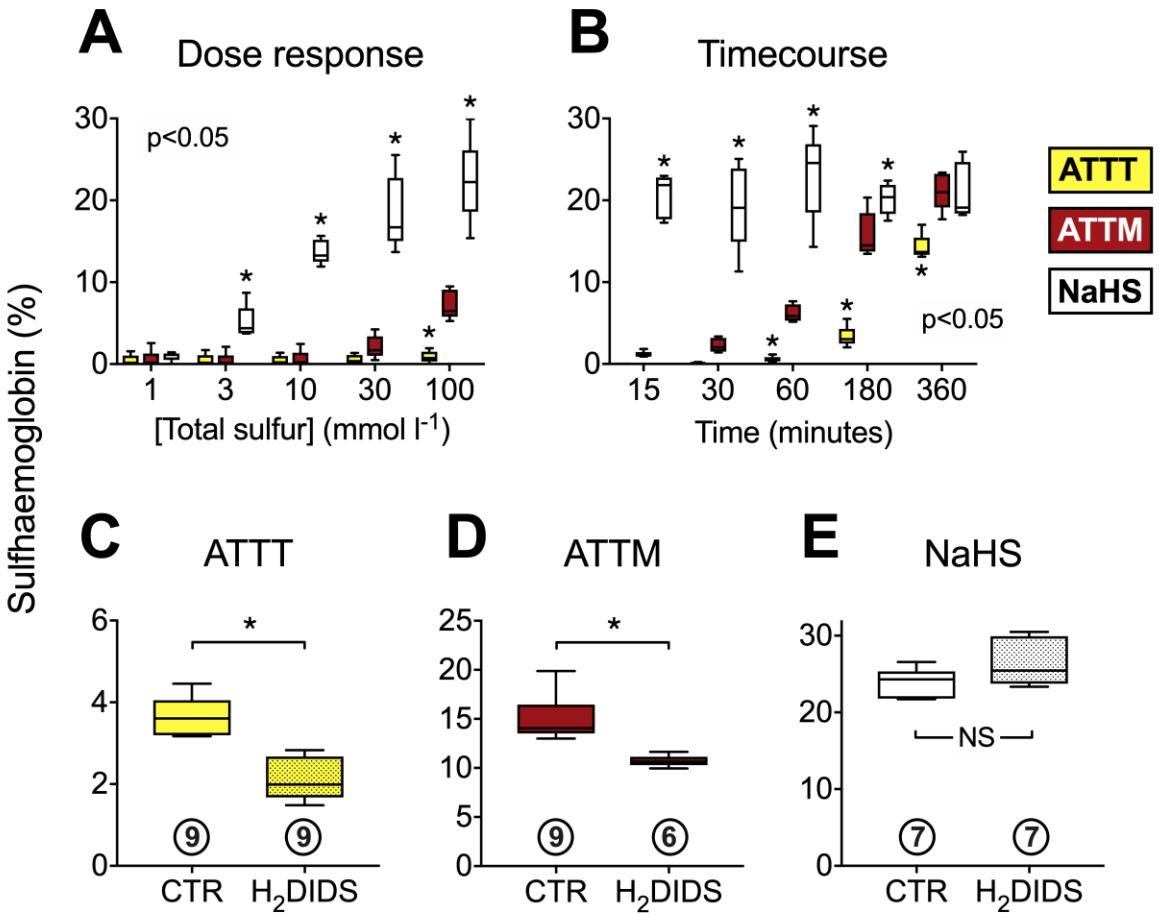

Fig 4. Formation of sulfhaemoglobin in human erythrocytes. A dose response (incubation for 1h) and time course (all drugs at 100 mmol l^{-1} total sulfur) are shown in (A) and (B), respectively; all n=5. The sensitivity of sulfhaemoglobin formation to (30 mins) pre-treatment with the anion exhanger-1 inhibitor (H_2DIDS; 4'diisothiocyanatodihydrostilbene-2,2'-disulfonic Acid; 0.5 mmol l^{-1}) is shown in panels (C-E). Sample sizes are shown in circles beneath each data set. Total sulfur for each drug was 100 mmol l^{-1}. Incubation time was 3h for the thiometallates (in C and D) and 15 mins for NaHS (E). Statistics: (A and B) 2-way ANOVA followed by Bonferroni's test. Stated p-values are the result of overall ANOVA. *p<0.05 vs ATTM (multiple comparisons). C-E, *p<0.05, unpaired non-parametric T-test. NS; not significant.

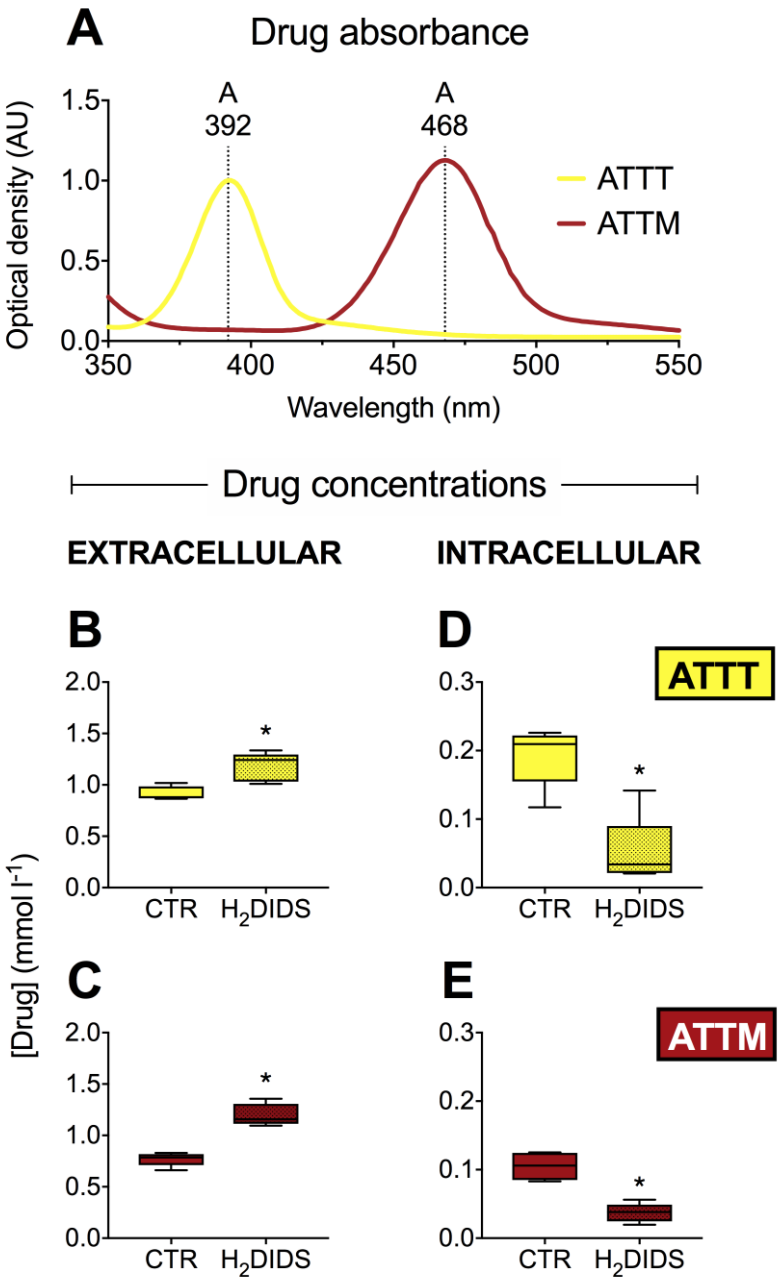

Fig 5. Extra- and intracellular concentrations of thiometallates. Absorbance spectrum of ATTT and ATTM is shown in (A) with λ_{MAX} values of 392 and 468 nm, respectively. Drug concentrations detected extracellularly are shown in panels (B) and (C) (both n=5). Corresponding intracellular measurements are shown in (D) and (E) (both n=5). H_2DIDS; 4'diisothiocyanatodihydrostilbene-2,2'-disulfonic Acid; 0.5 mmol l^{-1}). *p<0.05, non-parametric unpaired T-tests.

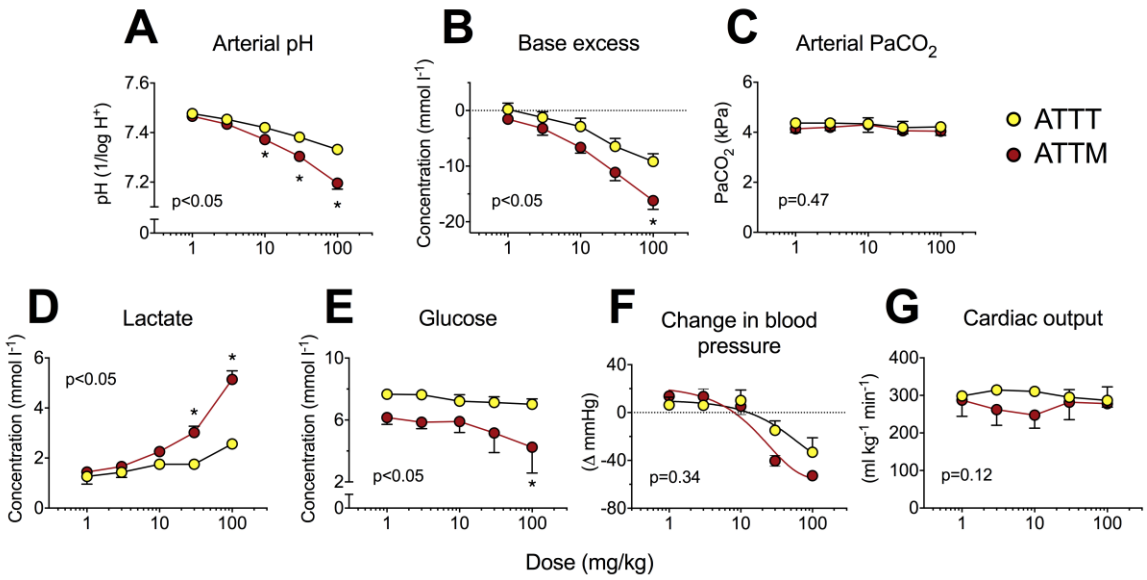

Fig 6. In vivo pharmacology of thiometallates. Panels (A-C) concern acid/base interactions with (A) arterial pH, (B) base excess (the metabolic component of acid/base status) and (C) arterial partial pressure of carbon dioxide ($PaCO_2$; respiratory component). Blood lactate and glucose levels are shown in (D) and (E), respectively. (F) shows maximal changes in mean arterial blood pressure for each dose while (G) depicts cardiac output, measured by echocardiographic pulsed-wave Doppler. Group sizes: n=6 for ATTT and n=5 for ATTM. *p<0.05; two-way repeated measures ANOVA followed by Bonferroni's test. Stated p-values are the result of the overall ANOVA.

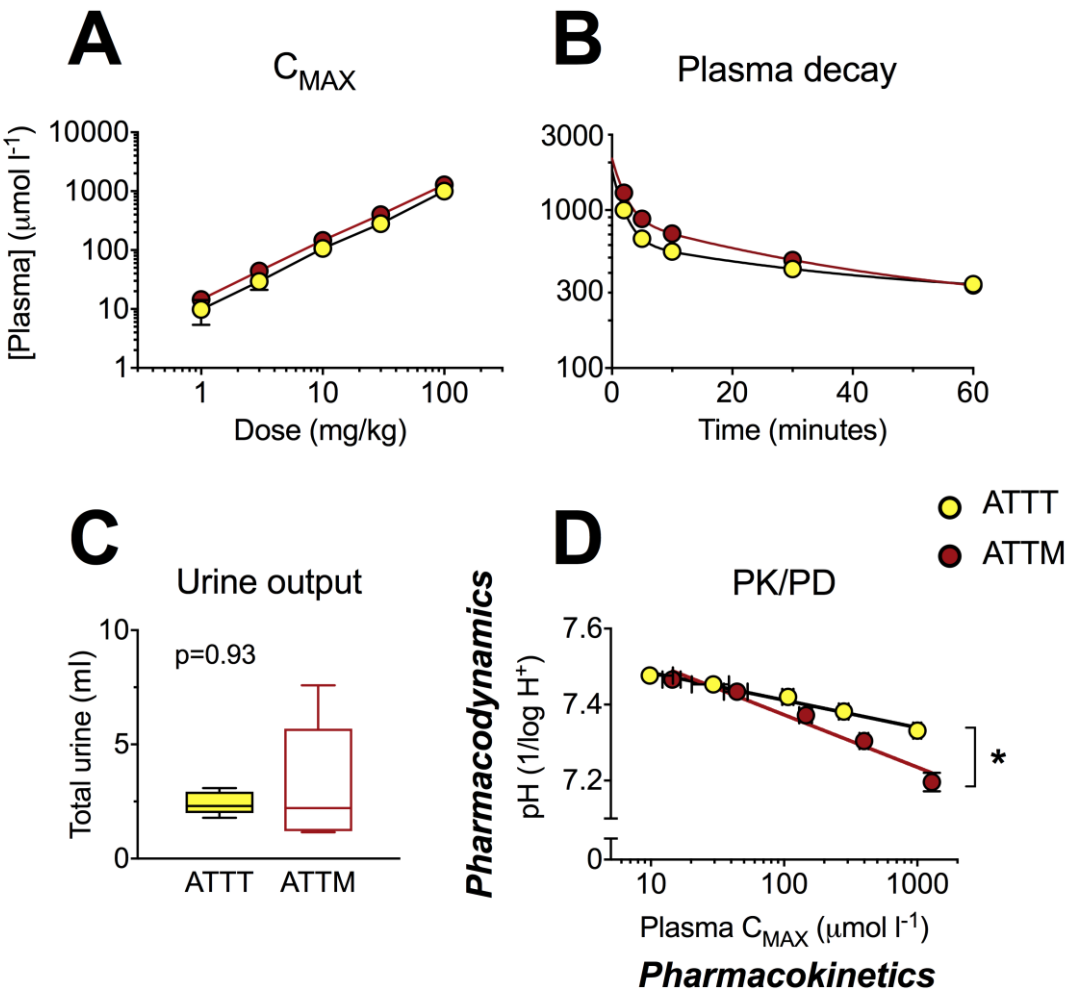

Fig 7. Pharmacokinetics. (A) shows the dependence of plasma concentration on IV dose level and (B) the decay in drug levels after the highest dose (100 mg kg^{-1}). (C) shows urine output. NB, the number of moles in urine was the same for both compounds (data not shown). (D) depicts the relationship between drug plasma levels (measured at 2 mins post-administration) and subsequent (25 mins later) changes in arterial pH. The slope in (D) is used as a surrogate for drug potency. Group sizes: n=6 for ATTT and n=5 for ATTM. *p<0.05; unpaired non-parametric T-test (urine output and slope in D).